

# Coupling Electrocatalysis and Biotransformation for CO<sub>2</sub>-Based Biomanufacturing

Huijuan Cui <sup>1</sup>, Xuan Wang <sup>2</sup> and Lingling Zhang <sup>1,3,\*</sup>

<sup>1</sup> State Key Laboratory of Engineering Biology for Low-Carbon Manufacturing, Tianjin Institute of Industrial Biotechnology, Chinese Academy of Sciences, Tianjin 300308, China; cuihj@tib.cas.cn (H.C.)

<sup>2</sup> College of Biotechnology, Tianjin University of Science & Technology, Tianjin 300457, China; wangxuan0222@163.com (X.W.)

<sup>3</sup> University of Chinese Academy of Sciences, Beijing 100049, China

\* Corresponding author. E-mail: zhangll@tib.cas.cn (L.Z.)

Received: 19 May 2025; Accepted: 10 June 2025; Available online: 18 June 2025

**ABSTRACT:** Transformation of CO<sub>2</sub> into high-value, long-chain carbon compounds is a long-term goal for CO<sub>2</sub> conversion and utilization. Electrocatalytic CO<sub>2</sub> reduction can achieve C1/C2 products with a high formation rate, while biosynthesis can utilize these C1/C2 species as substrates for carbon chain elongation. Coupling these two processes offers a promising avenue for efficient CO<sub>2</sub> fixation via synergizing the advantages of both sides. However, it is still challenging to realize its widespread application because of the poor compatibility between different modules. This review summarizes and discusses current developments in electrocatalytic-biosynthetic hybrid systems for CO<sub>2</sub> upcycling. First, the recent advances of individual modules are introduced, including conversion pathways, representative electrocatalysts and typical reactors for electrocatalytic CO<sub>2</sub> reduction process and microbial synthesis and *in vitro* multi-enzyme cascade catalysis for low-carbon bio-conversion process. Then, key factors that influence system coupling are discussed via analyzing the features of single modules and their cross-interference effects. Finally, several construction strategies are proposed based on different integration scenarios, offering guidance for the design and optimization of these hybrid systems.

**Keywords:** CO<sub>2</sub> upcycling; Electrocatalytic-biosynthetic hybrid systems; Electrocatalytic CO<sub>2</sub> reduction; Biological C1/C2 utilization



© 2025 The authors. This is an open access article under the Creative Commons Attribution 4.0 International License (<https://creativecommons.org/licenses/by/4.0/>).

## 1. Introduction

The excessive emission of carbon dioxide (CO<sub>2</sub>) has led to a series of serious environmental issues, including global warming, ocean acidification, and increased frequency of extreme weather events. Tackling this challenge requires not only reducing emissions but also actively converting CO<sub>2</sub> into value-added products. Past decades have achieved great progress in CO<sub>2</sub> transformation, including electro-, photo-, thermo-, and bio-approaches [1–7]. Among them, the electrochemical route is particularly promising for practical applications due to its operation under mild conditions and high product formation rates [7–9]. However, the major products of the electrocatalytic CO<sub>2</sub> reduction reaction (ECO<sub>2</sub>RR) are C1 and C2 species, such as CO, methane, formic acid, methanol, ethanol, ethylene, and acetic acid [10–13]. A long-term goal is direct CO<sub>2</sub> utilization to produce long-chain products, yet it is challenging due to the high C-C coupling energy barrier. Biocatalysis can utilize C1/C2 species as substrates to produce long-chain carbon products [14–17]. However, it is still difficult for high-efficiency fixation of CO<sub>2</sub> with direct bio-catalysis. One of the fundamental challenges of CO<sub>2</sub> fixation is its thermodynamic stability. CO<sub>2</sub> is a highly oxidized, low-energy molecule, and its conversion to more reduced forms (such as sugars, organic acids, or alcohols) requires a significant energy input. Many biological CO<sub>2</sub> fixation pathways (e.g., the Calvin-Benson-Bassham cycle) operate close to thermodynamic equilibrium, which leads to low driving forces and slow reaction rates. Key CO<sub>2</sub>-fixing enzymes such as RuBisCO, formate dehydrogenase (FDH), or carbon monoxide dehydrogenase often suffer from poor kinetics, oxygen sensitivity, or instability under industrial conditions [18,19]. For instance, most formate dehydrogenases such as *Cn*FDH, *Ec*FDH, and *Rc*FDH have low turnover rates and are prone to oxidation processes, which reduces carbon fixation efficiency

[20–22]. In anaerobic systems, many CO<sub>2</sub>-reducing enzymes are sensitive to O<sub>2</sub>, posing challenges for operation under ambient air conditions. Coupling electrocatalysis with biosynthesis for CO<sub>2</sub> fixation offers a powerful hybrid strategy that combines the strengths of both systems to overcome the limitations of each. By integrating these two approaches, the system enables stepwise carbon upgrading, improves overall energy and carbon efficiency, and expands the range of producible compounds. Moreover, the modularity of this hybrid design allows for flexible operation, better adaptation to intermittent renewable energy inputs, and the potential for carbon-negative production, making it a highly promising solution for sustainable biomanufacturing and CO<sub>2</sub> utilization.

Till now, several kinds of products have been synthesized via electrocatalytic-biosynthetic hybrid systems, such as glucose, fatty acid, bioplastics, and single cell protein [23–26]. Though remarkable achievements, the current coupling systems still face common challenges like insufficient energy conversion efficiency and sluggish transformation kinetics that are closely related to the compatibility and adaptability between different modules. Therefore, a timely and comprehensive review devoted to electrocatalytic-biosynthetic hybrid systems for CO<sub>2</sub> upcycling is beneficial to promote further development for CO<sub>2</sub> upcycling.

In this review, we focus on the latest advances in coupling electrocatalysis and biosynthesis for CO<sub>2</sub> fixation. We aim to provide a better understanding of the compatibility and adaptability between electrocatalysis and biosynthesis modules and guide the construction of electrocatalytic-biosynthetic hybrid systems. First, the progress achieved in each individual module is outlined respectively. Then, the key factors that would affect the integration of electrocatalytic and biosynthetic processes are discussed in detail via single-module and cross-interference analysis. Finally, several coupling strategies are proposed to guide the construction of hybrid systems.

## 2. Electrocatalytic CO<sub>2</sub> Reduction to C1/C2 Products

Electrocatalytic CO<sub>2</sub> reduction is a process that uses electricity to convert CO<sub>2</sub> into valuable chemicals and fuels. It possesses the advantages of high reaction rates, environmental friendliness, mild conditions, and ease of integration, showing promising prospects in CO<sub>2</sub> catalytic conversion. In this section, we introduce the latest advancements in electrocatalytic CO<sub>2</sub> reduction, mainly focusing on conversion pathways, representative electrocatalysts, and typical reactors.

### 2.1. Conversion Pathways and Representative Electrocatalysts

ECO<sub>2</sub>RR occurs at the electrode-electrolyte interface and involves multiple proton–electron transfer steps. Depending on the number of electrons transferred, a variety of reduction products can be obtained, including CO, formate, methane, methanol, ethylene, and ethanol [7,12,27–29]. The typical reaction pathways and key intermediates for the formation of C1 and C<sub>2+</sub> products are illustrated in Figure 1. There are two rate determining steps for CO formation: (1) \*COOH intermediate is formed via a concerted proton–electron transfer, and (2) the used electrocatalysts have appropriate adsorption strengths for CO, allowing for easy desorption from the electrode surface. Gold (Au) and silver (Ag) are commonly used as catalysts for CO production [30,31]. Different from CO, the common intermediate for HCOOH formation is HCOO\*, with two oxygen atoms binding on the surface of the electrocatalyst. Bismuth (Bi), tin (Sn), and indium (In)-based catalysts are typically employed for formate/formic acid generation [10,32–34]. Compared to multi-electron transfer processes, two-electron products like CO and formate are more readily formed, with selectivity up to 90% under industrial-level current densities [35,36].

Six electrons are needed to reduce CO<sub>2</sub> to methanol, for which \*CO and \*CHO are two key intermediates [29,37–39]. Cobalt phthalocyanine molecules anchored on carbon nanotubes can catalyse CO<sub>2</sub> reduction into methanol [29,39,40]. Improving stability in this reaction is a challenging requirement for practical application. Copper (Cu)-based catalysts are the most extensively studied for the conversion of CO<sub>2</sub> into C<sub>2+</sub> products such as ethanol, ethylene, and acetate [41–44]. The precise control of C–C coupling is one of the biggest challenges for ECO<sub>2</sub>RR due to the complexity of the intermediates. It is generally believed that the binding strength of CO with the metal surface plays a key role in forming C<sub>2+</sub> products. Optimal CO affinity can promote the formation of key intermediates of \*CO, \*CHO and \*COH, which further polymerize to generate C<sub>2+</sub> products [45–49]. At the current stage, the selectivity for C<sub>2+</sub> products remains below 70% and typically results in mixtures of multiple species. A deeper understanding of electrocatalytic mechanisms and the rational design of electrocatalysts are essential to improve overall performance in ECO<sub>2</sub>RR.

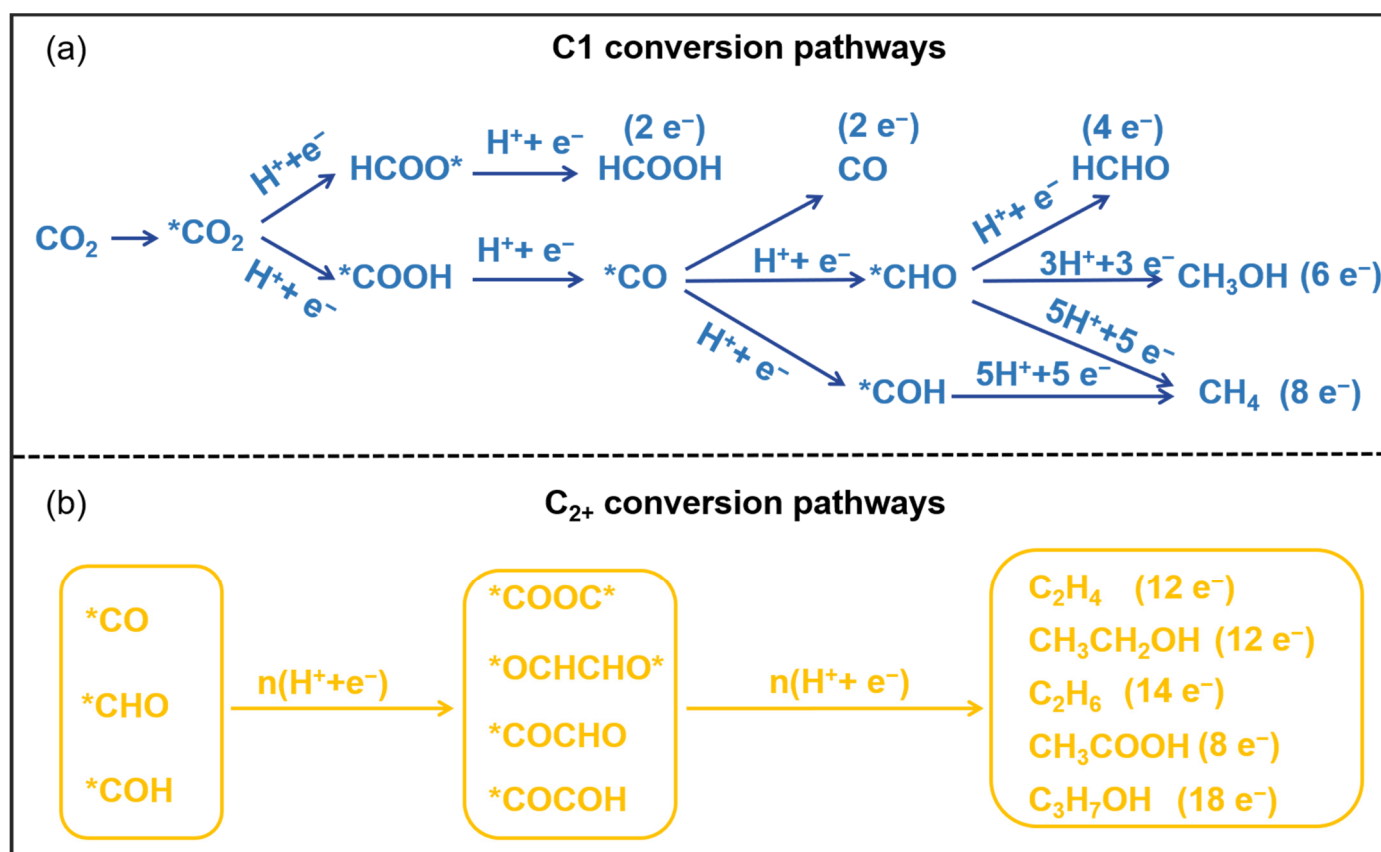


**Figure 1.** (a) The typical conversion routes and key intermediates for C1 products. (b) The typical conversion routes and key intermediates for C<sub>2+</sub> products.

Energy efficiency (EE) is a key performance metric for practical implementation, defined as the ratio of the chemical energy stored in products to the total electrical energy input. Recent years have seen substantial progress in improving the EE of ECO<sub>2</sub>RR, driven by advances in catalyst design, electrode architecture, and system engineering [50–55]. CO and formate production can now reach energy efficiencies exceeding 50%, while multi-carbon product formation still typically falls in the 20–40% range due to greater overpotentials and lower selectivity. Continued progress will rely on the co-development of catalysts, reactors, and integrated systems to achieve economically viable and sustainable CO<sub>2</sub> electrolysis.

## 2.2. Electrocatalytic Reactors

There are typically four types of electrocatalytic reactors used for ECO<sub>2</sub>RR: H-cell, flow cell, membrane electrode assembly cell (MEA) and solid-state electrolyte cell (Figure 2). The H-cell is a traditional three-electrode system consisting of working and reference electrodes in the cathode chamber and a counter electrode in the anode chamber, separated by an ion-exchange membrane. In this configuration, the substrate should be the dissolved CO<sub>2</sub> in the catholyte. Due to the inadequate solubility of CO<sub>2</sub> with regard to the high electrocatalytic performance of the electrocatalysts in aqueous solutions, the resulting current densities are typically moderate, making the H-cell more suitable for fundamental mechanistic studies rather than practical applications. In contrast, flow cells use a hydrophobic gas diffusion electrode (GDE) to separate the CO<sub>2</sub> gas from the catholyte, enabling the reaction to occur at the gas–liquid–solid triple-phase boundary [56,57]. This configuration significantly alleviates the gas diffusion limitation, allowing for higher current densities compared to H-cells. Water flooding of GDEs is one challenging problem in flow cells. Polytetrafluoroethylene (PTFE) can be used to modify the GDEs to prevent electro-wetting. Fang et al. reprocessed the GDE using a PTFE emulsion every 200 h, which effectively suppressed water flooding [58]. The fabricated device was stably operated for 5200 h at 2.2 V and a current density of 600 mA cm<sup>−2</sup>. MEA cells further improve performance by using humidified CO<sub>2</sub> without requiring a liquid catholyte on the cathode side. This setup reduces internal cell resistance and overcomes water flooding [59,60]. A low local pH can inhibit carbonate formation but accelerate H<sub>2</sub> generation. Such trade-offs highlight the importance of balancing pH effects. In solid state electrolyte cells, ion-conducting solid polymers are used to transport electrogenerated cations or anions to form electrolyte-free liquid products, avoiding energy-intensive downstream separation [61–64]. Xia et al. employed a solid-state electrolyte in a

ECO<sub>2</sub>RR system, realizing continuous conversion of CO<sub>2</sub> to pure HCOOH solution with concentrations up to 12 M [64]. Improving the conductivity of solid polymer is needed to decrease the cell voltage further and enhance the total energy efficiency in solid state electrolyte cells.

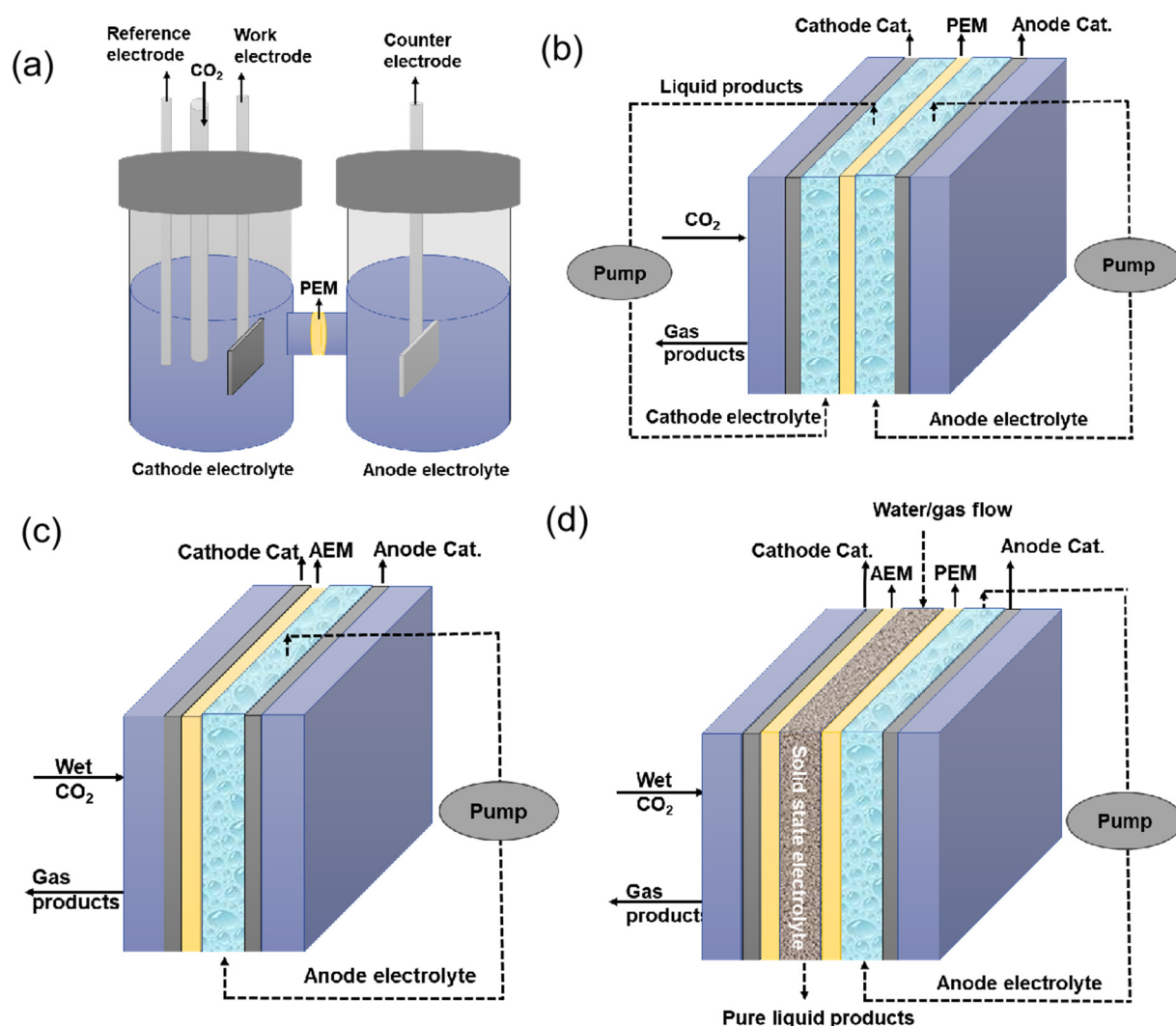


**Figure 2.** The schematic diagrams of electrocatalytic reactors for ECO<sub>2</sub>RR. (a) H-cell, (b) flow cell, (c) membrane electrode assembly cell and (d) Solid-state electrolyte cell.

### 3. Biosynthesis for Carbon Chain Elongation

Low-carbon biosynthesis, using short-chain carbon species as feedstocks and engineered biological systems as biotools for material processing and manufacturing, is an effective mode for carbon chain elongation [65,66]. Multiple products, such as biofuels, bioplastics and biomedicines, can be synthesized via this technology. In this section, recent progress of low-carbon biosynthesis is discussed from two aspects: microbial synthesis and *in vitro* multi-enzyme cascade catalysis.

#### 3.1. Multi-Enzyme Cascade Reaction

A cascade of enzymatic reactions can be integrated into complex biochemical pathways to enable carbon chain elongation, thereby enhancing the value-added potential of the final products [67–70]. Methanol can be synthesized from CO<sub>2</sub> via a multi-enzymatic cascade reaction of FDH, formaldehyde dehydrogenase (FaldDH), and alcohol dehydrogenase (ADH) [70,71]. In these processes, the conversion of HCOOH to HCHO is the rate-determining step due to its unfavorable thermodynamics. Searching for high-activity FaldDH is still challenging at the current stage. Similarly, dihydroxyacetone (DHA) can be achieved from CO<sub>2</sub> via cascading FDH, FaldDH, and formolase (FLS) (Figure 3a) [67]. A 1.8-fold increase in yield was achieved via immobilization of the used enzymes in hydrogen-bonded organic framework. Suitable immobilization can increase the local concentration of intermediates, improve mass

transfer efficiency and enhance enzyme stability [71,72]. Seo et al. designed a three-enzyme cascade reaction to produce 3-hydroxypropionaldehyde from methanol and ethanol [73]. A novel soluble alcohol oxidase HpAO<sub>x</sub> was used to convert methanol and ethanol into formaldehyde and acetaldehyde, which were subsequently condensed by 2-deoxyribose-5-phosphate aldolase. Together with a hydrogen peroxide elimination system based on a catalase, 3-hydroxypropionaldehyde was produced at a concentration of 18.3 mM from alcohols. Computational pathway design, modular assembly and substitution, and protein engineering of bottleneck-associated enzymes are effective strategies to enhance the performance of cascade reactions and achieve long-chain products [74,75]. Using these strategies, Cai et al. constructed a chemical-biochemical hybrid pathway for starch synthesis from CO<sub>2</sub>, consisting of 11 core reactions [74]. Methanol obtained via thermocatalytic hydrogenation of CO<sub>2</sub> served as a substrate for enzymatic reaction units. Lou et al. designed a non-natural *in vitro* multi-enzyme system for converting glycerol and CO<sub>2</sub> into L-aspartic acid [76]. The system utilized eight enzymes to convert the raw materials into L-aspartic acid in one-pot coupled with NADH and ATP regeneration. Under optimal reaction conditions, 18.6 mM of L-aspartic acid could be produced within 2 h at a total enzyme addition of 4.85 mg/mL. Ding et al. constructed three non-natural multienzyme cascade pathways for the synthesis of L-, D- and racemic lactic acid from renewable C1 methanol [77]. The methanol to lactic acid pathways contain 5–6 enzymatic steps involving 7–8 enzymes. Through enzyme assembly, modification, and optimization, lactic acid was produced from 100 mM methanol at a titer of 2.2–2.8 g/L.

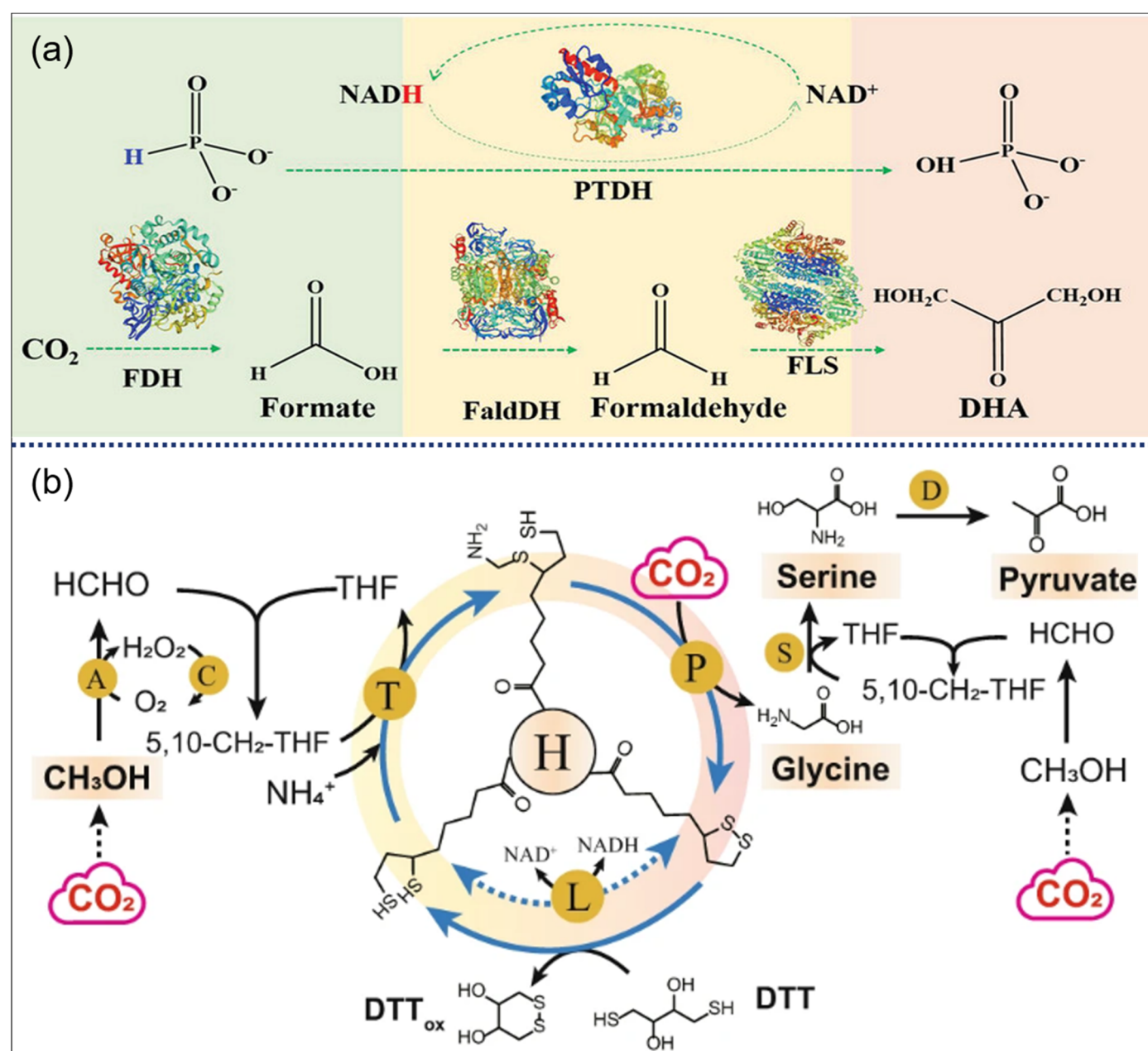


**Figure 3.** (a) Schematic illustration of conversion of CO<sub>2</sub> into dihydroxyacetone via a multi-enzyme cascade pathway [67]. Abbreviations: FDH formate dehydrogenase, FaldDH formaldehyde dehydrogenase, FLS formolase, PTDH phosphite



dehydrogenase, NADH reduced form of nicotinamide-adenine dinucleotide. Copyright © 2023 Wiley-VCH GmbH. **(b)** The reaction system to convert CO<sub>2</sub> and methanol into C2 glycine, C3 serine and pyruvate [78]. DTT is used to replace the function of L protein. Abbreviations: T aminomethyltransferase, P glycine decarboxylase, L dihydrolipoamide dehydrogenase, H aminomethyl carrier protein, A alcohol oxidase, S serine hydroxymethyltransferase, D L-serine deaminase. Copyright © 2023, The Author(s).

In these cascade reactions, cofactors such as NAD(H) and NADP(H) are usually added to supply the reducing equivalents required for the reaction [70,71]. Regeneration and reuse of cofactor should be considered due to their high cost. Enzymes like phosphite dehydrogenase (PTDH) and glutamate dehydrogenase (GDH) can be used for cofactor regeneration [67,70,71]. Except for enzymatic methods, these cofactors can also be continuously regenerated at the electrode surface using an external electric potential, which helps maintain a steady supply in enzymatic processes [79,80]. Electro-regenerated cofactors are typically classified as direct electrochemical regeneration and indirect electrochemical regeneration based on the mode of electron transfer between the electrode and the cofactor. For the former, the cofactor is regenerated directly at the electrode surface, which needs to shorten the distance between the electrode and the oxidation state of the cofactor. For the latter, a redox mediator is used to shuttle electrons between the electrode and the cofactor, such as viologens, quinones, or ferrocene derivatives. The redox potential of the selected mediator must match with that of cofactors. Wu et al. constructed an *in vitro* multi-enzymatic cascade based on the reductive glycine pathway, which realized glycine synthesis with CO<sub>2</sub> and NH<sub>3</sub> as the sole carbon and nitrogen sources [81]. Through effective coupling and the optimization of electrochemical cofactor regeneration and the multienzymatic cascade reaction, 0.81 mM glycine was yielded with the highest reaction rate of 8.69 mgL<sup>-1</sup>h<sup>-1</sup>. Li et al. developed a one-pot bioelectrochemical system featuring a rhodium-based catalyst which concurrently catalyzed gas-phase reduction of CO<sub>2</sub> to formate and NADH regeneration [82]. The bifunctional Rh<sup>III</sup>-complex cooperated with enzymatic cascades to produce dihydroxyacetone and L-erythrose with yields of 2.63 and 1.93 mM, respectively. Similarly, Luan et al. prepared ethylene glycol from CO<sub>2</sub> with a rhodium-based NADH regeneration electrode and a multi-enzymatic cascade system [68].

Other forms of energy, such as optical energy and chemical energy, can also be used to regenerate cofactors [68,78,83]. Ning et al. constructed a light-powered *in vitro* synthetic enzymatic biosystem to produce 3-Hydroxypropionic acid (3-HP) through CO<sub>2</sub> fixation from acetate [83]. The system employed natural thylakoid membranes (TMs) for the regeneration of ATP and NADP. Following optimization, production of 0.46 mM 3-HP was achieved within 6 h from an initial 0.5 mM acetate, with a yield nearing 92%. Additionally, reducing equivalents of cofactors can be replaced by chemical reductants due to their higher thermodynamic driving force. Liu et al. presented an ATP and NAD(P)H-free chemoenzymatic system for amino acid and pyruvate biosynthesis by coupling methanol with CO<sub>2</sub> (Figure 3b) [78]. Biocompatible chemical reduction of protein H with dithiothreitol was used to substitute for the NAD(P)H-dependent L protein in the re-engineered glycine cleavage system, achieving the synthesis of glycine, serine and pyruvate at the g/L level.

### 3.2. C1/C2 Assimilation via Microorganisms

Long-chain products can be efficiently synthesized through microbial pathways using short-chain carbon species as substrates [14,17,66,84–87]. The major natural carbon assimilation pathways are illustrated in Figure 4. For instance, formate can be assimilated via the Wood–Ljungdahl pathway (WLP) and the reductive glycine pathway (rGlyP), while methanol and formaldehyde serve as suitable substrates in the serine cycle, the ribulose monophosphate (RuMP) cycle, and the xylulose monophosphate (XuMP) cycle. Acetyl-CoA is usually a hub metabolite in these central metabolic pathways. Realize the high-efficiency synthesis of Acetyl-CoA is of great importance. Compared to natural metabolic pathways, synthetic metabolic pathways have the advantages of customizability and flexibility, which can meet specific production goals and improve the flux of metabolites [15]. As a result, increasing attention has been directed toward the design and construction of synthetic pathways [88–90]. Common strategies include pathway design, gene engineering, expression tuning, and dynamic regulation to balance and enhance metabolic flux.

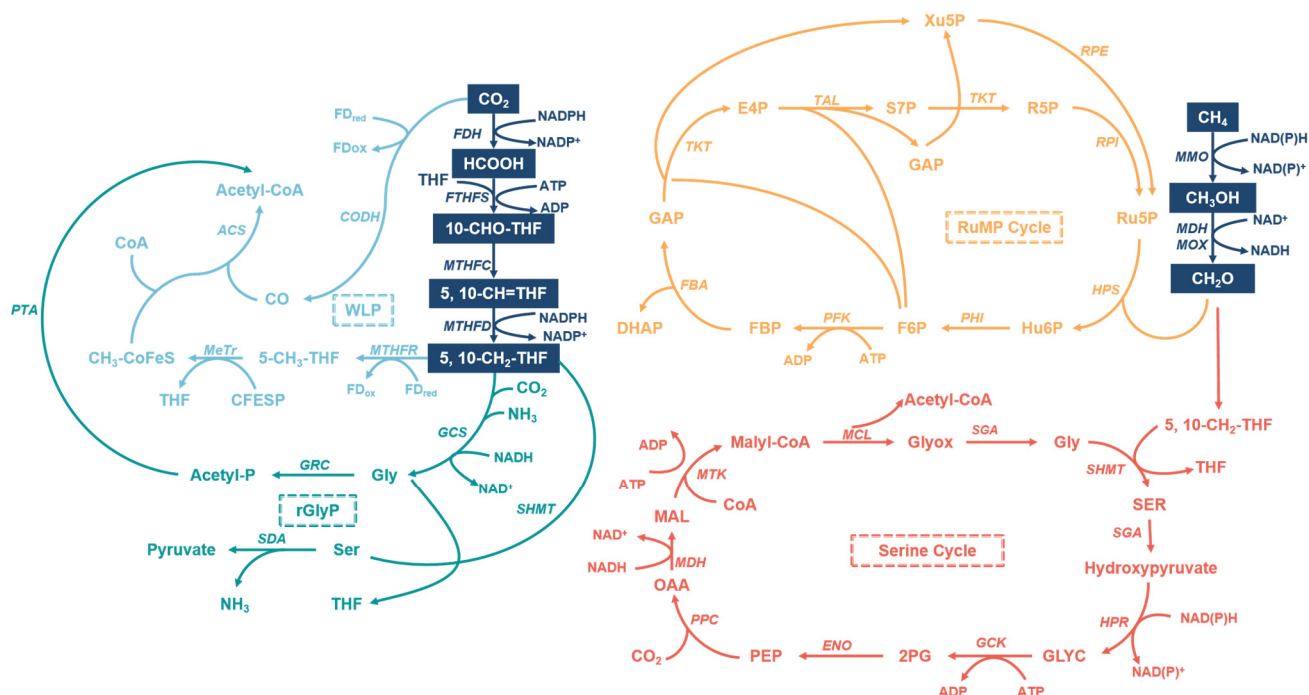
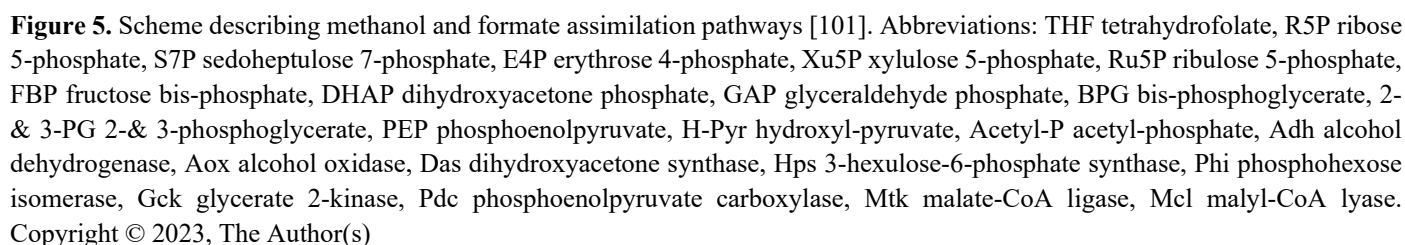


**Figure 4.** The typical nature assimilation pathways of short-chain carbon species.

Gas substrates such as CO and methane can also be used for biosynthesis [91,92]. The low solubility of these species in water is one of the major challenges to their utilization. Ma et al. developed a novel bioreactor configuration, in which a hollow fiber membrane was used for efficient methane supply while microorganisms were growing in the suspended form favourable for biomass harvest [92]. Under the optimal conditions, long-term experiments demonstrated excellent single cell protein production, with yields of 1.36 g/g methane and high protein content of up to 67%. Compared to gas species, liquid substrates such as formate, methanol, acetate, and ethanol are more favorable for utilization. Among them, methanol is a promising sole carbon source for microbial cell factories due to its high storage capacity and the availability of regulatable metabolic pathways [88,93–95]. Zhao et al. synthesized cordycepin using *Pichia pastoris* with methanol as a carbon source, achieving titers of 1.55 g/L in shake-flask fermentation and 8.11 g/L in fed-batch fermentation [96]. Similarly, Niu et al. reprogrammed the metabolic network of *P. pastoris* to convert methanol into the sesquiterpene phytoalexin zealexin A1 [97]. Formaldehyde, a key intermediate in methylotrophic microorganisms, can be generated through the reduction of formate or the oxidation of methanol [89,98]. However, due to its instability and toxicity, formaldehyde is typically treated as a transient intermediate rather than a direct substrate, emphasizing the need to finely balance its upstream synthesis and downstream conversion [98]. Formate is another C1 substrate that can be utilized by microorganisms [99]. However, native formate-assimilating strains generally exhibit sluggish growth and limited efficiency, particularly when formate is used as the sole carbon source. Substrate co-utilization has emerged as an effective strategy to enhance carbon fixation efficiency [90,100–102]. For instance, Tian et al. engineered a *Vibrio natriegens* strain with a heterologous indigoidine biosynthetic pathway, achieving 29.0 g/L of indigoidine and consuming 165.3 g/L of formate over 72 h through co-utilization of formate and glucose [102]. In another study, Bernd et al. discovered and validated an oxygen-tolerant reductive glycine pathway capable of co-assimilating methanol, formate, and CO<sub>2</sub> in the yeast *Komagataella phaffii*, highlighting the potential of industrially relevant microorganisms for one-carbon fixation (Figure 5) [101]. C2 species such as acetate and ethanol can be converted to acetyl-CoA in two to three steps and enter primary metabolism rapidly to serve as energy sources and metabolic building blocks [24,84,86,103–108]. Feng et al. synthesized phenol from acetate using engineered *Escherichia coli* [84]. Through fed-batch fermentation combined with *in situ* extraction, the phenol titer was raised to 2.01 g/L. Qian et al. reassembled the *S. baicalensis* 4'-deoxyflavone biosynthetic pathway in *Pichia pastoris*, producing 4'-deoxyflavones [108]. Synthetic transcriptional devices were designed to regulate the five splitting pathway modules, enabling high-level *de novo* baicalein production.



Electrocatalytic-biosynthetic coupled CO<sub>2</sub> fixation is an emerging approach that combines electrocatalysis with biological processes to convert CO<sub>2</sub> into valuable chemicals and fuels. Electrocatalysis provides a controlled, renewable energy-driven CO<sub>2</sub> conversion process, while biosynthesis enables the production of complex, high-value compounds with high selectivity. The combination enhances overall efficiency and product diversity, potentially leading to a sustainable circular carbon economy. In this section, we focus on analyzing and discussing the key factors that influence



effective integration, and based on the latest developments, we propose several potential strategies for constructing integrated systems.

#### 4.1. Key Factors for Effective Coupling

Only effective coupling can fully leverage the advantages of the electrocatalysis module and the biosynthesis module, achieving efficient CO<sub>2</sub> fixation. Consequently, a thorough analysis and discussion of the key factors influencing this hybridization is necessary. These potential influencing factors are summarized in Figure 6.

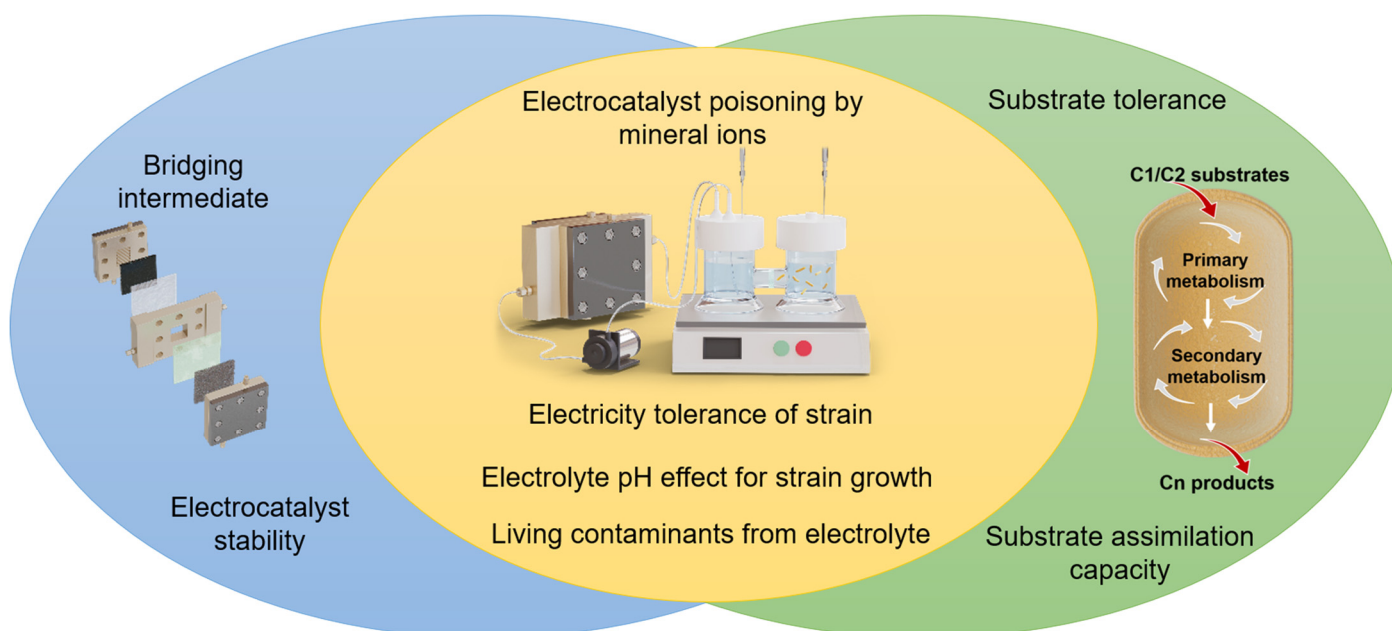


**Figure 6.** The possible factors that have significant influence on coupling.

In the electrocatalysis module, the selection of appropriate bridging intermediates is crucial. Compared to gaseous products such as CO and methane, liquid products are more suitable for subsequent biosynthesis, as they avoid the limitations associated with low gas solubility. From a technological maturity standpoint, ECO<sub>2</sub>RR for formate production is currently the most feasible for industrial-scale applications, owing to its significantly higher selectivity and formation rates compared to C<sub>2+</sub> products. Other liquid products, such as methanol, ethanol, and acetate, possess higher energy content and are also advantageous for biological utilization. However, improving their selectivity and yield remains an urgent challenge. Another critical factor is the stability of electrocatalysts. Biosynthetic processes typically require tens to hundreds of hours to complete a single production batch. Most reported electrocatalysts for ECO<sub>2</sub>RR fail to maintain performance over such extended periods, which poses a significant barrier to practical application, particularly in ready-to-use systems. Strategies such as surface modification, alloying, support engineering, and optimization of operating conditions have shown promise in enhancing electrocatalyst stability [10,109,110].

Substrate tolerance and substrate assimilation capacity are two key points in biocatalytic module. The former determines the upper limit of substrate concentration in biosynthesis, while the latter determines the lower limit of substrate concentration. Excessive accumulation of substrates such as formaldehyde and methanol may poison the enzymes or cells, even leading to cell death; likewise, when substrates are too scarce, the enzymatic reaction may not occur, and the microorganisms may stop growing or even die. Adaptive laboratory evolution is an effective approach to enhance the substrate tolerance of strains. Using this strategy, an evolved strain of *Vibrio natriegens* was capable of growing in the presence 140 g L<sup>-1</sup> sodium formate [102]. Metabolic engineering can be used to improve the metabolic efficiency of substrate assimilation pathways. Common strategies include optimization of pathway gene expression levels, engineering of key pathway enzymes, blocking of competing pathways, reconstruction of cofactor regeneration systems, and modular optimization of metabolic pathways. Wang et al. introduced a bacterial ribulose monophosphate (RuMP) pathway in addition to the native xylulose monophosphate (XuMP) pathway of *P. pastoris*, creating a hybrid network that significantly improved erythritol production and reduced pentitol byproduct formation [95]. Tan et al. engineered a channel-modulating helix of formolase to fine-tune the shape of the substrate/product channel [111]. The activity of the best variant was enhanced by 27.3-fold at 20 mM formaldehyde and 86.5-fold at 40 mM formaldehyde

compared to the starting point, which increased the availability of substrate formaldehyde to promote the formation of C3 product 1,3-dihydroxyacetone.

Cross-interference effects between electrocatalytic and biocatalytic modules are the most critical factors limiting their effective integration. When the culture medium is directly used as the catholyte, the mineral ions it contains, such as  $\text{Ca}^{2+}$  and  $\text{Mg}^{2+}$  ions, may lead to electrocatalyst deactivation during electroreduction; the electric field in the electrocatalysis module may kill strains or enzymes with low electrical tolerance; electrocatalysts typically exhibit higher activity under strongly alkaline conditions, but excessively high pH can impair the activity of biocatalysts; primary or secondary metabolites might react at the electrode surface, decreasing the titer of final products; the electrocatalysis module operates as a semi-open system, which may introduce contamination risks when integrated with the biological module. Only when these cross-interference issues are resolved can we achieve the ready-to-use state of bridging intermediates; otherwise, a spatiotemporally separated coupled system is required.

#### 4.2. Achievements in Electrocatalysis-Biosynthesis Hybrid Systems

With advances in both  $\text{ECO}_2\text{RR}$  and biological C1/C2 utilization, electrocatalytic–biosynthetic hybrid systems for carbon fixation have emerged and achieved notable progress (Table 1) [23–25,112–114]. For example, Zheng et al. developed a hybrid electro-biosystem that couples spatially separated  $\text{CO}_2$  electrolysis with yeast fermentation to efficiently convert  $\text{CO}_2$  into glucose [23]. Pure acetic acid was produced from  $\text{CO}_2$  via a two-step electrocatalysis with a solid-electrolyte reactor. *Saccharomyces cerevisiae* was engineered to produce glucose *in vitro* from electro-generated acetic acid by deleting all defined hexokinase genes and overexpression of heterologous glucose-1-phosphatase. Similarly, Hann et al. developed a hybrid inorganic-biological artificial photosynthesis system for energy-efficient food production [112]. Gong et al. achieved succinic acid from  $\text{CO}_2$  via combining processes of  $\text{ECO}_2\text{RR}$  and microbial synthesis [115]. In their system, Cu-organic framework catalyst was first synthesized for electrocatalytic conversion of  $\text{CO}_2$  to ethanol via a solid-state electrolyte cell. Subsequently, an engineered *E. coli* was used to assimilate the  $\text{CO}_2$ -derived ethanol to produce succinic acid. After engineering optimization, the succinic acid titer reached 53.8 mM with a yield of 0.41 mol/mol, 82% of the theoretical yield. Liu et al. coupled photovoltaics-powered electrocatalysis with a five-enzyme cascade platform engineered through genetic mutation and bioinformatics (Figure 7) [116]. This system realized the conversion of  $\text{CO}_2$  to L-sorbose with a solar-to-food energy conversion efficiency of 3.5%.

**Table 1.** Key performance metrics for representative coupled electrocatalytic-biosynthetic systems.

Number	$\text{ECO}_2\text{RR}$ Process				Biosynthetic Process					
	Products	Electrocatalyst	FE	EE <sub>1</sub>	Strain/Enzyme	Products	Titer/ (g/L)	Productivity/ (g/L/h)	EE <sub>2</sub>	Total EE
1 [23]	acetic acid	Ni single atom catalyst/Cu	46%	6.52%	<i>S. cerevisiae</i>	glucose	1.81	0.009	10%	0.65%
2 [112]	acetate	Ag/Cu	57%	39.37%	<i>C. reinhardtii</i>	algae	0.29	0.0015	41.75	16.4%
3 [115]	ethanol	Cu-MOF	84.7%		<i>E. coli</i>	succinic acid	6.35	0.42		
4 [116]	formate	Bi-nanowire	82.2%		Multi-enzymes <sup>a</sup>	L-sorbose	9.6	0.1		22.6%
5 [24]	C <sub>2+</sub>	Cu	24.9%	13.6%	<i>P. putida</i>	PHA <sup>b</sup> /biomass	0.56	0.023	21.9%	3%
6 [25]	formate	Cu/Cu <sub>2</sub> O	55%	19.3%	<i>P. communis</i>	SCP <sup>c</sup>	2.6	0.06	47.7%	9.2%
7 [114]	formate	Sn catalysts	66%		<i>C. necator</i>	PHB <sup>d</sup>	0.69	0.006		

Notes a: the used enzymes include formaldehyde dehydrogenase, phosphite dehydrogenase, aldolase, D-fructose-6-phosphatase aldolase, and A129S mutant of aldolase. b: PHA is polyhydroxyalkanoates. c: SCP is single cell protein. d: PHB is poly-3-hydroxybutyrate.

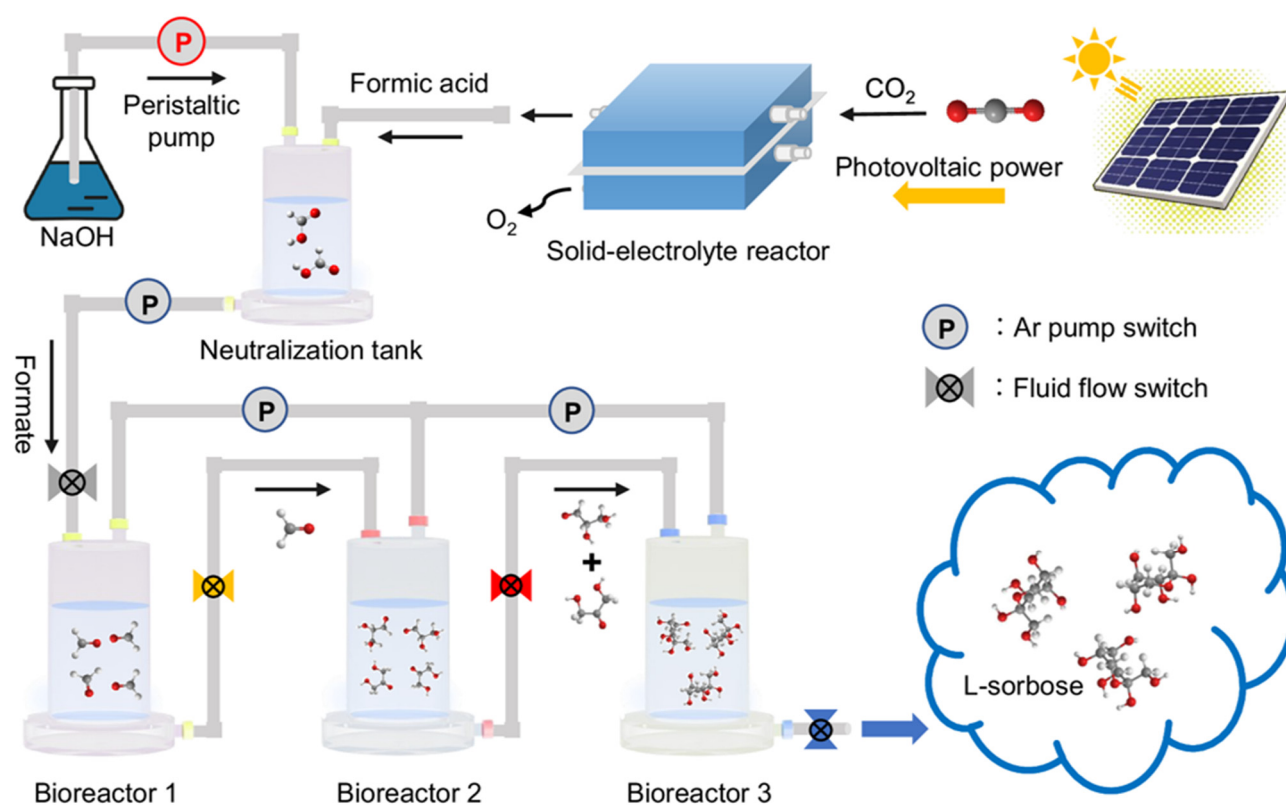


**Figure 7.** Electrocatalytic–biocatalytic flow system, in which CO<sub>2</sub> was first converted into formate by photovoltaics-powered electrocatalysis, followed by direct injection of produced formate into designed tandem bioreactors for food production [116]. Copyright © 2024, The Author(s)

Once the cross-interference issues between the electrocatalytic and biocatalytic modules are resolved, fully integrated, ready-to-use systems can be established [24,25,117]. For example, installing an anion exchange membrane on the electrocatalyst surface can effectively separate mineral ions from the culture medium, minimizing their interference. Additionally, employing a two-chamber design with a filter membrane in the biosynthesis module can protect microbial cells from the adverse effects of electrocatalysis. Zhang et al. utilized these strategies realizing production of PHA from CO<sub>2</sub> (Figure 8a) [24]. In their system, Cu was used as electrocatalyst to produce ethanol and acetate, which served as intermediates for *Pseudomonas putida* utilization. Cui et al. coupled an ECO<sub>2</sub>RR to formate module with a formate assimilation module, achieving single cell protein with CO<sub>2</sub> as the sole carbon source (Figure 8b) [25]. Strain adaptability investigation and equipment upgrading were carried out to guarantee effective integration. The growth rate and electrical energy conversion efficiency were reached up to 0.114 OD h<sup>−1</sup> and 9.2%, respectively. Chen et al. designed an electro-biodiesel route via integrating ECO<sub>2</sub>RR and bioconversion through biocompatible C<sub>2+</sub> intermediates [117]. Bioenergetic and metabolic limits in C<sub>2+</sub> intermediate utilization were revealed through simulations and metabolomics, guiding the synthetic biology design to achieve reductant balance, more ATP production, efficient lipid conversion, and higher lipid yield. Lim et al. reported the integration of CO<sub>2</sub> electrolysis with microbial fermentation to directly produce PHB [114]. This biohybrid system comprised electrochemical conversion of CO<sub>2</sub> to formate on Sn-based catalysts and subsequent conversion of formate to PHB by *Cupriavidus necator* cells in a fermenter. After system optimization, PHB was accumulated in *C. necator* cells with a content of 83% of dry cell weight.

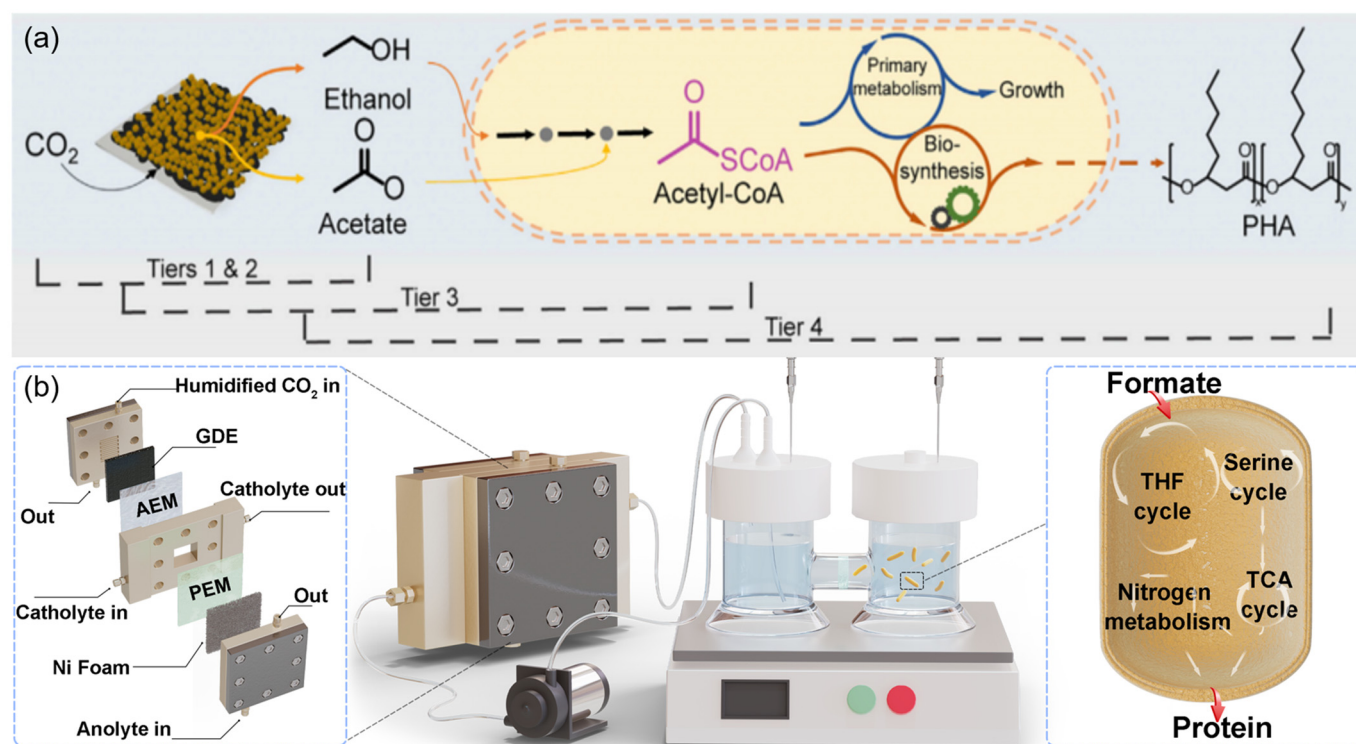


**Figure 8.** (a) The schematic illustration of four-tier design for polyhydroxyalkanoates production [24]. Copyright © 2022 The Authors. (b) Schematic diagram of the electrocatalytic-biosynthetic integrated system for single cell protein production [25]. Copyright © 2024 Elsevier B.V.

#### 4.3. Strategies for Devices Design

Selecting appropriate devices to construct a coupling system is crucial for overcoming mismatches between different modules and enhancing overall carbon fixation efficiency. We systematically analyzed the factors affecting the coupling process through both single-module and cross-interference evaluations. Based on these insights, we propose several coupling strategies, as illustrated in Figure 9.

For the electrocatalytic module, a single membrane flow cell system—where a cation exchange membrane separates the cathode and anode chambers—is suitable when electrocatalyst has high compatibility with the biosynthesis module (Figure 9a). That is, the electrode surface exhibits high anti-pollution capacity, which is not easily polluted or poisoned by microorganisms or mineral ions in the culture medium. Adding a cation exchange membrane on the surface of the cathode catalyst can effectively suppress the interference of cations in the culture medium with the electrocatalyst's activity, making it suitable for systems where the culture medium is directly used as the catholyte (Figure 9b). Solid-state electrolyte cells can produce pure liquid products that can be directly fed into the biosynthesis module (Figure 9c). However, the relatively low conductivity of solid-state electrolytes results in reduced energy conversion efficiency. Further optimization of solid-state electrolyte performance could significantly enhance the overall energy efficiency.

For the biosynthesis module, it is essential to fully consider the factors such as voltage, pH, temperature and salt tolerance of the biocatalysts. During electrocatalysis, the electrode surface usually possesses higher pH and temperature than the bulk solution, especially when running under high voltage. The local high pH and temperature may lead to inactivation of biocatalysts. High voltages can lead to the formation of reactive oxygen species such as superoxide anions, hydrogen peroxide, and hydroxyl radicals. These species can oxidatively damage proteins, lipids, DNA, and other cellular components, leading to loss of enzymatic activity or cell viability. Strong electric fields can disrupt the tertiary and quaternary structures of enzymes, altering the configuration of their active sites and resulting in irreversible loss of function. In microbial systems, high voltage can compromise cell membrane integrity, leading to leakage of cellular contents, disruption of ion gradients, and eventual cell lysis. Several strategies can be attempted to mitigate these issues. Redox mediators facilitate electron transfer between electrodes and biocatalysts, allowing operation at lower voltages that are less damaging to biological components. Embedding enzymes or microbes in protective matrices can buffer them against electric fields and reactive oxygen species. Modifying electrode surfaces with biocompatible



coatings can reduce local electric field intensity and reactive oxygen species production. When the biocatalysts are highly compatible with the electrocatalysis module, a single-chamber synthesis module can be directly integrated with the electrocatalysis module (Figure 9d). If the strain has low tolerance for voltage, pH and temperature, a dual-chamber fermenter can be used to separate the microorganisms from the electrocatalytic module via a filter (Figure 9e). In cases where there is strong cross-interference between the electrocatalytic and biosynthesis modules, a fully spatially separated fermentation system may be employed (Figure 9f). For example, when primary/secondary metabolites decompose at the electrode surface, this fully spatially separated system is needed.

When the metabolic rate of microorganisms surpasses the rate of electrochemical production—as in the case of methanol production and utilization—two strategic approaches can be considered. The first involves developing highly efficient electrocatalysts and designing electrochemical stack systems in series or parallel configurations to enhance methanol yield through ECO<sub>2</sub>RR. The second strategy focuses on ensuring an adequate methanol supply by coupling electrocatalytic hydrogen production with thermocatalytic CO<sub>2</sub> hydrogenation. Both technologies are advancing rapidly and show strong potential to meet the demands of methanol utilization.

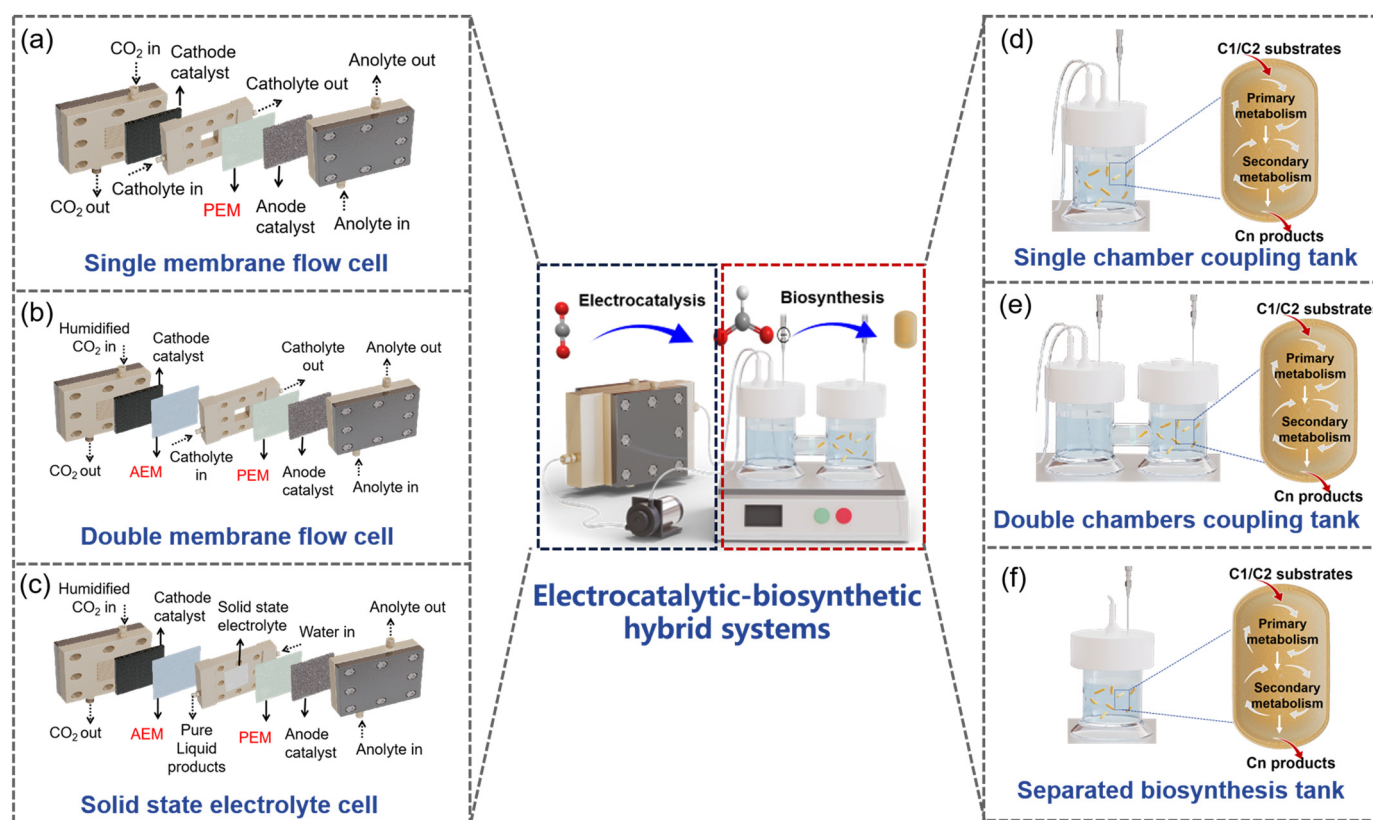


**Figure 9.** Possible routes for constructing electrocatalysis-biosynthesis coupling systems. (a–c) The schematic illustration of possible devices used in electrocatalytic module. (a) Single membrane flow cell, (b) double membrane flow cell, and (c) solid state electrolyte cell. (d–f) The schematic illustration of possible tanks used in biosynthetic module. (d) Single chamber coupling tank, (e) double chambers coupling tank, and (f) separated biosynthesis tank.

## 5. Conclusions and Perspectives

Coupling ECO<sub>2</sub>RR with biosynthesis is a promising strategy for CO<sub>2</sub> upcycling. However, mismatches between the electrocatalytic and biosynthetic modules hinder efficiency. In this review, we systematically analyze factors affecting this coupled process through single-module and cross-interference evaluations. Based on our analysis and discussion, we propose several coupling strategies: a single membrane flow cell with a single chamber tank suits systems with minimal cross-interference; a double membrane flow cell helps mitigate mineral ion effects on electrocatalysts; a dual-chamber tank with a filter isolates microbial strains from voltage interference; and a solid-state electrolyte cell delivers pure solutions directly to bioreactors, enabling spatiotemporally separated systems.

Although significant progress has been made, such investigations are still in their infancy, with many challenges yet to face. In the electrocatalytic module, the current energy efficiency is relatively low, with full-cell energy efficiencies generally below 50%. This is one of the main reasons for the low energy efficiency of the coupling systems.



The issue is directly related to the excessively high reaction over-potential. Accelerating proton-coupled electron transfer via optimizing the structure and composition of electrocatalysts is a potential strategy to reduce the over-potential. In the biosynthesis module, the slow growth and limited metabolic capacity of native C1/C2-utilizing strains are key bottlenecks hindering high-efficiency coupling. Laboratory adaptive evolution and metabolic engineering tailored to specific strains can enhance their substrate assimilation capacity. At the system integration level, overcoming cross-interference between different modules is crucial. Artificial intelligence modeling and thermodynamic simulations can help to predict potential coupling conditions, which facilitate optimization of system integration, thereby improving overall performance.

### Author Contributions

Conceptualization, H.C. and L.Z.; Writing—Original Draft Preparation, H.C. and X.W.; Writing—Review & Editing, H.C. and L.Z.; Supervision, L.Z.; Funding Acquisition, L.Z.

### Ethics Statement

Not applicable.

### Informed Consent Statement

Not applicable.

### Funding

This work was supported by the Strategic Priority Research Program of the Chinese Academy of Sciences XDC0120103 and CAS Project for Young Scientists in Basic Research YSBR 072-3.

### Declaration of Competing Interest

The authors declare that they have no known competing financial interests or personal relationships that could have appeared to influence the work reported in this paper.

### References

- Ren G, Wei Z, Liu S, Shi M, Li Z, Meng X. Recent review of  $\text{Bi}_x\text{MO}_y$  ( $M = \text{V}, \text{Mo}, \text{W}$ ) for photocatalytic  $\text{CO}_2$  reduction into solar fuels. *Chemosphere* **2022**, 307, 136026. doi:10.1016/j.chemosphere.2022.136026.
- Mehla S, Kandjani AE, Babarao R, Lee AF, Periasamy S, Wilson K, et al. Porous crystalline frameworks for thermocatalytic  $\text{CO}_2$  reduction: an emerging paradigm. *Energy Environ. Sci.* **2021**, 14, 320–352. doi:10.1039/d0ee01882a.
- Zhang C, Lin Z, Jiao L, Jiang H-L. Metal-organic frameworks for electrocatalytic  $\text{CO}_2$  reduction: from catalytic site design to microenvironment modulation. *Angew. Chem. Int. Ed.* **2024**, 63, e202414506. doi:10.1002/anie.202414506.
- Tang Z, Liu X, Yang Y, Jin F. Recent advances in  $\text{CO}_2$  reduction with renewable reductants under hydrothermal conditions: towards efficient and net carbon benefit  $\text{CO}_2$  conversion. *Chem. Sci.* **2024**, 15, 9927–9948. doi:10.1039/d4sc01265h.
- Dang H, Guan B, Chen J, Ma Z, Chen Y, Zhang J, et al. Research status, challenges, and future prospects of carbon dioxide reduction technology. *Energy Fuels* **2024**, 38, 4836–4880. doi:10.1021/acs.energyfuels.3c04591.
- Xia Q, Yang J, Hu L, Zhao H, Lu Y. Biotransforming  $\text{CO}_2$  into valuable chemicals. *J. Clean Prod.* **2024**, 434, 140185. doi:10.1016/j.jclepro.2023.140185.
- Cui H, Guo Y, Guo L, Wang L, Zhou Z, Peng Z. Heteroatom-doped carbon materials and their composites as electrocatalysts for  $\text{CO}_2$  reduction. *J. Mater. Chem. A* **2018**, 6, 18782–18793. doi:10.1039/c8ta07430e.
- Nitopi S, Bertheussen E, Scott SB, Liu X, Engstfeld AK, Horch S, et al. Progress and perspectives of electrochemical  $\text{CO}_2$  reduction on copper in aqueous electrolyte. *Chem. Rev.* **2019**, 119, 7610–7672. doi:10.1021/acs.chemrev.8b00705.
- Woldu AR, Huang Z, Zhao P, Hu L, Astruc D. Electrochemical  $\text{CO}_2$  reduction ( $\text{CO}_2\text{RR}$ ) to multi-carbon products over copper-based catalysts. *Coord. Chem. Rev.* **2022**, 454, 214340. doi:10.1016/j.ccr.2021.214340.
- Li W, Yu C, Tan X, Ren Y, Zhang Y, Cui S, et al. Beyond leverage in activity and stability toward  $\text{CO}_2$  electroreduction to formate over a bismuth catalyst. *ACS Catal.* **2024**, 14, 8050–8061. doi:10.1021/acscatal.4c01519.
- Chang B, Min Z, Liu N, Wang N, Fan M, Fan J, et al. Electrocatalytic  $\text{CO}_2$  reduction to syngas. *Green Energy Environ.* **2024**, 9, 1085–1100. doi:10.1016/j.gee.2023.05.005.
- Yu S, Yamauchi H, Wang S, Aggarwal A, Kim J, Gordiz K, et al.  $\text{CO}_2$ -to-methanol electroconversion on a molecular cobalt catalyst facilitated by acidic cations. *Nat. Catal.* **2024**, 7, 1000–1009. doi:10.1038/s41929-024-01197-2.

13. Guo Y, Yao S, Xue Y, Hu X, Cui H, Zhou Z. Nickel single-atom catalysts intrinsically promoted by fast pyrolysis for selective electroreduction of CO<sub>2</sub> into CO. *Appl. Catal. B-Environ.* **2022**, *304*, 120997. doi:10.1016/j.apcatb.2021.120997.
14. Kim Y, Lee SH, Gade P, Nattermann M, Maltseva N, Endres M, et al. Revealing reaction intermediates in one-carbon elongation by thiamine diphosphate/CoA-dependent enzyme family. *Commun. Chem.* **2024**, *7*, 160. doi:10.1038/s42004-024-01242-y.
15. Yang X, Zhang Y, Zhao G. Artificial carbon assimilation: from unnatural reactions and pathways to synthetic autotrophic systems. *Biotech. Adv.* **2024**, *70*, 108294. doi:10.1016/j.biotechadv.2023.108294.
16. O’Keeffe S, Garcia L, Chen Y, Law RC, Liu C, Park JO. Bringing carbon to life via one-carbon metabolism. *Trends Biotechnol.* **2025**, *43*, 572–585. doi:10.1016/j.tibtech.2024.08.014.
17. Müller M, Germer P, Andexer JN. Biocatalytic One-carbon transfer-a review. *Synthesis* **2022**, *54*, 4401–4425. doi:10.1055/s-0040-1719884.
18. Mulder DW, Peters JW, Raugei S. Catalytic bias in oxidation-reduction catalysis. *Chem. Commun.* **2021**, *57*, 713–720. doi:10.1039/d0cc07062a.
19. Adamson H, Robinson M, Wright JJ, Flanagan LA, Walton J, Elton D, et al. Retuning the catalytic bias and overpotential of a [NiFe]-hydrogenase via a single amino acid exchange at the electron entry/exit site. *J. Am. Chem. Soc.* **2017**, *139*, 10677–10686. doi:10.1021/jacs.7b03611.
20. Yu X, Niks D, Mulchandani A, Hille R. Efficient reduction of CO<sub>2</sub> by the molybdenum-containing formate dehydrogenase from *Cupriavidus necator* (*Ralstonia eutropha*). *J. Biol. Chem.* **2017**, *292*, 16872–16879. doi:10.1074/jbc.M117.785576.
21. Bassegoda A, Madden C, Wakeley DW, Reisner E, Hirst J. Reversible interconversion of CO<sub>2</sub> and formate by a molybdenum-containing formate dehydrogenase. *J. Am. Chem. Soc.* **2014**, *136*, 15473–15476. doi:10.1021/ja508647u.
22. Hartmann T, Leimkühler S. The oxygen-tolerant and NAD<sup>+</sup>-dependent formate dehydrogenase from *Rhodobacter capsulatus* is able to catalyze the reduction of CO<sub>2</sub> to formate. *FEBS J.* **2013**, *280*, 6083–6096. doi:10.1111/febs.12528.
23. Zheng T, Zhang M, Wu L, Guo S, Liu X, Zhao J, et al. Upcycling CO<sub>2</sub> into energy-rich long-chain compounds via electrochemical and metabolic engineering. *Nat. Catal.* **2022**, *5*, 388–396. doi:10.1038/s41929-022-00775-6.
24. Zhang P, Chen K, Xu B, Li J, Hu C, Yuan JS, et al. Chem-bio interface design for rapid conversion of CO<sub>2</sub> to bioplastics in an integrated system. *Chem* **2022**, *8*, 3363–3381. doi:10.1016/j.chempr.2022.09.005.
25. Cui H, Liu W, Ma C, Shiri P, Zhu Z, Jiang H, et al. Converting CO<sub>2</sub> to single-cell protein via an integrated electrocatalytic-biosynthetic system. *Appl. Catal. B-Environ. Energy* **2024**, *350*, 123946. doi:10.1016/j.apcatb.2024.123946.
26. Pan Z, Guo Y, Rong W, Wang S, Cui K, Cai W, et al. Single-cell protein production from CO<sub>2</sub> and electricity with a recirculating anaerobic-aerobic bioprocess. *Environ. Sci. Ecotechnol.* **2025**, *24*, 100525. doi:10.1016/j.ese.2025.100525.
27. Cui H-f, Yang F, Liu C, Zhu H-w, Liu M-y, Guo R-t. Recent progress of covalent organic frameworks-based materials used for CO<sub>2</sub> electrocatalytic reduction: a review. *Small* **2025**, *21*, 2502867. doi:10.1002/smll.202502867.
28. Liu C, Guo R-t, Zhu H-w, Cui H-f, Liu M-y, Pan W-g. Cu<sub>2</sub>O-based catalysts applied for electrocatalytic CO<sub>2</sub> reduction: A review. *J. Mater. Chem. A* **2024**, *12*, 31769–31796. doi:10.1039/d4ta06287f.
29. Rooney CL, Lyons M, Wu Y, Hu G, Wang M, Choi C, et al. Active sites of cobalt phthalocyanine in electrocatalytic CO<sub>2</sub> reduction to methanol. *Angew. Chem. Int. Ed.* **2024**, *63*, e202310623. doi:10.1002/anie.202310623.
30. Souza ML, Lima FHB. Dibenzylidithiocarbamate-functionalized small gold nanoparticles as selective catalysts for the electrochemical reduction of CO<sub>2</sub> to CO. *ACS Catal.* **2021**, *11*, 12208–12219. doi:10.1021/acscatal.1c00591.
31. Iqbal MZ, Imteyaz S, Ghanty C, Sarkar S. A review on electrochemical conversion of CO<sub>2</sub> to CO: Ag-based electrocatalyst and cell configuration for industrial application. *J. Ind. Eng. Chem.* **2022**, *113*, 15–31. doi:10.1016/j.jiec.2022.05.041.
32. Lei PX, Liu SQ, Wen QR, Wu JY, Wu S, Wei X, et al. Integrated “two-in-one” strategy for high-rate electrocatalytic CO<sub>2</sub> reduction to formate. *Angew. Chem. Int. Ed.* **2024**, *64*, e202415726. doi:10.1002/anie.202415726.
33. Xue J, Fu X, Geng S, Wang K, Li Z, Li M. Boosting electrochemical CO<sub>2</sub> reduction via valence state and oxygen vacancy controllable Bi-Sn/CeO<sub>2</sub> nanorod. *J. Environ. Manag.* **2023**, *342*, 118354. doi:10.1016/j.jenvman.2023.118354.
34. Li P, Yang F, Li J, Zhu Q, Xu JW, Loh XJ, et al. Nanoscale engineering of p-block metal-based catalysts toward industrial-scale electrochemical reduction of CO<sub>2</sub>. *Adv. Energy Mater.* **2023**, *13*, 2301597. doi:10.1002/aenm.202301597.
35. Jin S, Hao Z, Zhang K, Yan Z, Chen J. Advances and challenges for the electrochemical reduction of CO<sub>2</sub> to CO: From fundamentals to industrialization. *Angew. Chem. Int. Ed.* **2021**, *60*, 20627–20648. doi:10.1002/anie.202101818.
36. Ye N, Wang K, Tan Y, Qian Z, Guo H, Shang C, et al. Industrial-level CO<sub>2</sub> to formate conversion on Turing-structured electrocatalysts. *Nat. Syn.* **2025**. doi:10.1038/s44160-025-00769-9.
37. Zhu Q, Rooney CL, Shema H, Zeng C, Panetier JA, Gross E, et al. The solvation environment of molecularly dispersed cobalt phthalocyanine determines methanol selectivity during electrocatalytic CO<sub>2</sub> reduction. *Nat. Catal.* **2024**, *7*, 987–999. doi:10.1038/s41929-024-01190-9.
38. Zhu N, Zhang X, Chen N, Zhu J, Zheng X, Chen Z, et al. Integration of MnO<sub>2</sub> nanosheets with Pd nanoparticles for efficient CO<sub>2</sub> electroreduction to methanol in membrane electrode assembly electrolyzers. *J. Am. Chem. Soc.* **2023**, *145*, 24852–24861. doi:10.1021/jacs.3c09307.

39. Wu Y, Jiang Z, Lu X, Liang Y, Wang H. Domino electroreduction of CO<sub>2</sub> to methanol on a molecular catalyst. *Nature* **2019**, 575, 639–642. doi:10.1038/s41586-019-1760-8.
40. Li J, Zhu Q, Chang A, Cheon S, Gao Y, Shang B, et al. Molecular-scale CO spillover on a dual-site electrocatalyst enhances methanol production from CO<sub>2</sub> reduction. *Nat. Nanotechnol.* **2025**, 20, 515–522. doi:10.1038/s41565-025-01866-8.
41. Wang H, Xue J, Liu C, Chen Z, Li C, Li X, et al. CO<sub>2</sub> electrolysis toward acetate: a review. *Curr. Opin. Electrochem.* **2023**, 39, 101253. doi:10.1016/j.coelec.2023.101253.
42. Yang B, Liu K, Li H, Liu C, Fu J, Li H, et al. Accelerating CO<sub>2</sub> electroreduction to multicarbon products via synergistic electric-thermal field on copper nanoneedles. *J. Am. Chem. Soc.* **2022**, 144, 3039–3049. doi:10.1021/jacs.1c11253.
43. Yang Y, Tan Z, Zhang J. Electrocatalytic carbon dioxide reduction to ethylene over copper-based catalytic systems. *Chem.-Asian J.* **2022**, 17, 202200893. doi:10.1002/asia.202200893.
44. Liu L-X, Qin C, Deng T, Sun L, Chen Z, Han X. Cu MOF-based electrocatalysts for CO<sub>2</sub> reduction to multi-carbon products. *J. Mater. Chem. A* **2024**, 12, 26421–26438. doi:10.1039/d4ta05059b.
45. Li Z, Liu Z, Li S, Pei Y, Li D, Mao J, et al. Modulating the localized electronic distribution of Cu species during reconstruction for enhanced electrochemical CO<sub>2</sub> reduction to C<sub>2+</sub> products. *J. Mater. Chem. A* **2024**, 12, 15082–15089. doi:10.1039/d4ta01184h.
46. Sun L, Zheng X, Li Y, Lin M, Zeng X, Yu J, et al. Nanoconfinement and tandem catalysis over yolk-shell catalysts towards electrochemical reduction of CO<sub>2</sub> to multi-carbon products. *J. Colloid Interface Sci.* **2025**, 687, 733–741. doi:10.1016/j.jcis.2025.02.089.
47. Ma X, Fang C, Ding M, Zuo Y, Sun X, Wang S. Atomic-level elucidation of lattice-hydrogens in copper catalysts for selective CO<sub>2</sub> electrochemical conversion toward C<sub>2</sub> products. *Angew. Chem. Int. Ed.* **2025**, 64, e202500191. doi:10.1002/anie.202500191.
48. Zhao Z-H, Ren D. Unravelling the effect of crystal facet of derived-copper catalysts on the electroreduction of carbon dioxide under unified mass transport condition. *Angew. Chem. Int. Ed.* **2025**, 64, e202415590. doi:10.1002/anie.202415590.
49. Subramanian S, Kok J, Gholkar P, Sajeev Kumar A, van Montfort H-PI, Kortlever R, et al. CO residence time modulates multi-carbon formation rates in a zero-gap Cu based CO<sub>2</sub> electrolyzer. *Energy Environ. Sci.* **2024**, 17, 6728–6738. doi:10.1039/d4ee02004a.
50. Cao C, Ma D-D, Gu J-F, Xie X, Zeng G, Li X, et al. Metal-organic layers leading to atomically thin bismuthene for efficient carbon dioxide electroreduction to liquid fuel. *Angew. Chem. Int. Ed.* **2020**, 59, 15014–15020. doi:10.1002/anie.202005577.
51. Wang Y, Li Y, Liu J, Dong C, Xiao C, Cheng L, et al. BiPO<sub>4</sub>-derived 2D nanosheets for efficient electrocatalytic reduction of CO<sub>2</sub> to liquid fuel. *Angew. Chem. Int. Ed.* **2021**, 60, 7681–7685. doi:10.1002/anie.202014341.
52. Edwards JP, Xu Y, Gabardo CM, Dinh C-T, Li J, Qi Z, et al. Efficient electrocatalytic conversion of carbon dioxide in a low-resistance pressurized alkaline electrolyzer. *Appl. Energy* **2020**, 261, 114305. doi:10.1016/j.apenergy.2019.114305.
53. Ozden A, Liu Y, Dinh C-T, Li J, Ou P, García de Arquer FP, et al. Gold adparticles on silver combine low overpotential and high selectivity in electrochemical CO<sub>2</sub> conversion. *ACS Appl. Energy Mater.* **2021**, 4, 7504–7512. doi:10.1021/acs.aem.1c01577.
54. O'Brien CP, Miao RK, Shayesteh Zeraati A, Lee G, Sargent EH, Sinton D. CO<sub>2</sub> Electrolyzers. *Chem. Rev.* **2024**, 124, 3648–3693. doi:10.1021/acs.chemrev.3c00206.
55. Lin L, He X, Xie S, Wang Y. Electrocatalytic CO<sub>2</sub> conversion toward large-scale deployment. *Chin. J. Catal.* **2023**, 53, 1–7. doi:10.1016/s1872-2067(23)64524-3.
56. Niu Z-Z, Chi L-P, Liu R, Chen Z, Gao M-R. Rigorous assessment of CO<sub>2</sub> electroreduction products in a flow cell. *Energy Environ. Sci.* **2021**, 14, 4169–4176. doi:10.1039/d1ee01664d.
57. Ma D, Jin T, Xie K, Huang H. An overview of flow cell architecture design and optimization for electrochemical CO<sub>2</sub> reduction. *J. Mater. Chem. A* **2021**, 9, 20897–20918. doi:10.1039/d1ta06101a.
58. Fang W, Guo W, Lu R, Yan Y, Liu X, Wu D, et al. Durable CO<sub>2</sub> conversion in the proton-exchange membrane system. *Nature* **2024**, 626, 86–91. doi:10.1038/s41586-023-06917-5.
59. Hu L, Wrubel JA, Baez-Cotto CM, Intia F, Park JH, Kropf AJ, et al. A scalable membrane electrode assembly architecture for efficient electrochemical conversion of CO<sub>2</sub> to formic acid. *Nat. Commun.* **2023**, 14, 7605. doi:10.1038/s41467-023-43409-6.
60. Ge L, Rabiee H, Li M, Subramanian S, Zheng Y, Lee JH, et al. Electrochemical CO<sub>2</sub> reduction in membrane-electrode assemblies. *Chem* **2022**, 8, 663–692. doi:10.1016/j.chempr.2021.12.002.
61. Wang Z, Zhou Y, Liu D, Qi R, Xia C, Li M, et al. Carbon-confined indium oxides for efficient carbon dioxide reduction in a solid-state electrolyte flow cell. *Angew. Chem. Int. Ed.* **2022**, 61, e202200552. doi:10.1002/anie.202200552.
62. Luthfiah A, Lee CW. Solid-state electrolyte-based electrochemical conversion of carbon dioxide: progress and opportunities. *Chemcatchem* **2023**, 15, e202300702. doi:10.1002/cctc.202300702.
63. Zheng T, Liu C, Guo C, Zhang M, Li X, Jiang Q, et al. Copper-catalysed exclusive CO<sub>2</sub> to pure formic acid conversion via single-atom alloying. *Nat. Nanotechnol.* **2021**, 16, 1386–1393. doi:10.1038/s41565-021-00974-5.
64. Xia C, Zhu P, Jiang Q, Pan Y, Liang W, Stavitsk E, et al. Continuous production of pure liquid fuel solutions via electrocatalytic CO<sub>2</sub> reduction using solid-electrolyte devices. *Nat. Energy* **2019**, 4, 776–785. doi:10.1038/s41560-019-0451-x.

65. Wang Q, Zhang Y, Tian C, Sun Z, Ma Y. Low-carbon biosynthesis: opportunities and challenges. *Chin. Sci. Bull.* **2023**, *68*, 2427–2434. doi:10.1360/tb-2022-1194.
66. Park W, Cha S, Hahn J-S. Advancements in biological conversion of C1 feedstocks: sustainable bioproduction and environmental solutions. *ACS Syn. Biol.* **2024**, *13*, 3788–3798. doi:10.1021/acssynbio.4c00519.
67. Pei R, Liu J, Jing C, Zhang M. A multienzyme cascade pathway immobilized in a hydrogen-bonded organic framework for the conversion of CO<sub>2</sub>. *Small* **2023**, *20*, 2306117. doi:10.1002/smll.202306117.
68. Luan L, Zhang Y, Ji X, Guo B, Song S, Huang Y, et al. Electro-driven multi-enzymatic cascade conversion of CO<sub>2</sub> to ethylene glycol in nano-reactor. *Adv. Sci.* **2024**, *11*, 2407204. doi:10.1002/advs.202407204.
69. Wang P, Wang X, Chandra S, Lielpetere A, Quast T, Conzuelo F, et al. Hybrid enzyme-electrocatalyst cascade modified gas-diffusion electrodes for methanol formation from carbon dioxide. *Angew. Chem. Int. Ed.* **2025**, *64*, e202422882. doi:10.1002/anie.202422882.
70. Singh RK, Singh R, Sivakumar D, Kondaveeti S, Kim T, Li J, et al. Insights into cell-free conversion of CO<sub>2</sub> to chemicals by a multienzyme cascade reaction. *ACS Catal.* **2018**, *8*, 11085–11093. doi:10.1021/acscatal.8b02646.
71. Zhu D, Ao S, Deng H, Wang M, Qin C, Zhang J, et al. Ordered coimmobilization of a multienzyme cascade system with a metal organic framework in a membrane: reduction of CO<sub>2</sub> to methanol. *ACS Appl. Mater. Interfaces* **2019**, *11*, 33581–33588. doi:10.1021/acsami.9b09811.
72. Di Spiridione C, Aresta M, Dibenedetto A. Improving the enzymatic cascade of reactions for the reduction of CO<sub>2</sub> to CH<sub>3</sub>OH in water: from enzymes immobilization strategies to cofactor regeneration and cofactor suppression. *Molecules* **2022**, *27*, 4913. doi:10.3390/molecules27154913.
73. Seo M-J, Jeong Y-J, Ju S-B, Kim D-M, Seo H-R, Son HF, et al. Enzymatic cascade transformation of renewable C1 and C2 alcohols into 3-Hydroxypropionaldehyde with a high conversion rate. *ACS Sustain. Chem. Eng.* **2025**, *13*, 2694–2705. doi:10.1021/acssuschemeng.4c07133.
74. Cai T, Sun H, Qiao J, Zhu L, Zhang F, Zhang J, et al. Cell-free chemoenzymatic starch synthesis from carbon dioxide. *Science* **2021**, *373*, 1523–1527. doi:10.1126/science.abh4049.
75. Yang J, Song W, Cai T, Wang Y, Zhang X, Wang W, et al. De novo artificial synthesis of hexoses from carbon dioxide. *Sci. Bull.* **2023**, *68*, 2370–2381. doi:10.1016/j.scib.2023.08.023.
76. Lou L, Cheng F, Li Z, Li Z. Constructing an artificial *in vitro* multi-enzyme cascade pathway to convert glycerol and CO<sub>2</sub> into L-aspartic acid. *Bioresour. Technol.* **2024**, *411*, 131350. doi:10.1016/j.biortech.2024.131350.
77. Ding X-W, Rong J, Pan Z-P, Zhu X-X, Zhu Z-Y, Chen Q, et al. De novo multienzyme synthetic pathways for lactic acid production. *ACS Catal.* **2024**, *14*, 4665–4674. doi:10.1021/acscatal.3c05489.
78. Liu J, Zhang H, Xu Y, Meng H, Zeng AP. Turn air-captured CO<sub>2</sub> with methanol into amino acid and pyruvate in an ATP/NAD(P)H-free chemoenzymatic system. *Nat. Commun.* **2023**, *14*, 2772. doi:10.1038/s41467-023-38490-w.
79. Li Y, Liu G, Kong W, Zhang S, Bao Y, Zhao H, et al. Electrocatalytic NAD(P)H regeneration for biosynthesis. *Green Chem. Eng.* **2024**, *5*, 1–15. doi:10.1016/j.gce.2023.02.001.
80. Lee YS, Gerulskis R, Minter SD. Advances in electrochemical cofactor regeneration: enzymatic and non-enzymatic approaches. *Curr. Opin. Biotechnol.* **2022**, *73*, 14–21. doi:10.1016/j.copbio.2021.06.013.
81. Wu R, Li F, Cui X, Li Z, Ma C, Jiang H, et al. Enzymatic electrosynthesis of glycine from CO<sub>2</sub> and NH<sub>3</sub>. *Angew. Chem. Int. Ed.* **2023**, *62*, e202218387. doi:10.1002/anie.202218387.
82. Li H, Wu Y, Wang Y, Zhang K, Zhu J, Ji Y, et al. Bifunctional RhIII-complex-catalyzed CO<sub>2</sub> reduction and NADH regeneration for direct bioelectrochemical synthesis of C3 and C4. *ACS Catal.* **2024**, *14*, 17201–17208. doi:10.1021/acscatal.4c05457.
83. Ning X, Li F, Wei X, Zhu Z, You C. A light-powered *in vitro* synthetic enzymatic biosystem for the synthesis of 3-hydroxypropionic acid via CO<sub>2</sub> fixation. *ACS Syn. Biol.* **2024**, *13*, 2611–2620. doi:10.1021/acssynbio.4c00447.
84. Feng J, Zhao Y, Liu Z, Wang X, Xu S, Chen K. Engineered biosynthesis of phenol using acetate as the carbon source in *Escherichia coli*. *ACS Sustain. Chem. Eng.* **2025**, *13*, 1657–1666. doi:10.1021/acssuschemeng.4c08437.
85. Lv X, Yu W, Zhang C, Ning P, Li J, Liu Y, et al. C1-based biomanufacturing: advances, challenges and perspectives. *Bioresour. Technol.* **2023**, *367*, 128259. doi:10.1016/j.biortech.2022.128259.
86. Bortolucci J, Zani ACB, de Gouvêa PF, Dinamarco TM, Reginatto V. A non-solventogenic *Clostridium beijerinckii* strain lacking acetoacetate decarboxylase assimilates acetate and accumulates butyrate. *Biomass Bioenerg.* **2023**, *172*, 106780. doi:10.1016/j.biombioe.2023.106780.
87. Li S, Liu Y, Gao Z, An C, Gu H, Yin H, et al. Methane valorization to antioxidant polysaccharides by methanotrophic bacteria. *J. Agric. Food Chem.* **2025**, *73*, 11019–11029. doi:10.1021/acs.jafc.5c01087.
88. Gan Y, Meng X, Gao C, Song W, Liu L, Chen X. Metabolic engineering strategies for microbial utilization of methanol. *Eng. Microbiol.* **2023**, *3*, 100081. doi:10.1016/j.engmic.2023.100081.
89. Wu T, Gómez-Coronado PA, Kubis A, Lindner SN, Marlière P, Erb TJ, et al. Engineering a synthetic energy-efficient formaldehyde assimilation cycle in *Escherichia coli*. *Nat. Commun.* **2023**, *14*, 8490. doi:10.1038/s41467-023-44247-2.

90. Bysani VR, Alam AS, Bar-Even A, Machens F. Engineering and evolution of the complete reductive glycine pathway in *Saccharomyces cerevisiae* for formate and CO<sub>2</sub> assimilation. *Metab. Eng.* **2024**, *81*, 167–181. doi:10.1016/j.ymben.2023.11.007.
91. Xu J, Wang J, Ma C, Wei Z, Zhai Y, Tian N, et al. Embracing a low-carbon future by the production and marketing of C1 gas protein. *Biotechnol. Adv.* **2023**, *63*, 108096. doi:10.1016/j.biotechadv.2023.108096.
92. Ma Y, Liu T, Yuan Z, Guo J. Single cell protein production from methane in a gas-delivery membrane bioreactor. *Water Res.* **2024**, *259*, 121820. doi:10.1016/j.watres.2024.121820.
93. Shen Y, Cai P, Gao L, Wu X, Yao L, Zhou YJ. Engineering high production of fatty alcohols from methanol by constructing coordinated dual biosynthetic pathways. *Bioresour. Technol.* **2024**, *412*, 131396. doi:10.1016/j.biortech.2024.131396.
94. Jiang W, Newell W, Liu J, Coppens L, Borah Slater K, Peng H, et al. Insights into the methanol utilization capacity of *Y. lipolytica* and improvements through metabolic engineering. *Metab. Eng.* **2025**, *91*, 30–43. doi:10.1016/j.ymben.2025.03.014.
95. Wang S, Fang J, Wang M, Yu S, Xia Y, Liu G, et al. Rewiring the methanol assimilation pathway in the methylotrophic yeast *Pichia pastoris* for high-level production of erythritol. *Bioresour. Technol.* **2025**, *427*, 132430. doi:10.1016/j.biortech.2025.132430.
96. Zhao B, Li Y, Zhang Y, Pan M, Zhao G, Guo Y. Low-carbon and overproduction of cordycepin from methanol using engineered *Pichia pastoris* cell factory. *Bioresour. Technol.* **2024**, *413*, 131446. doi:10.1016/j.biortech.2024.131446.
97. Niu T, Yan X, Wang J, Song H, Cui Y, Cai X, et al. Engineering of *Pichia pastoris* for the *de novo* synthesis of the desquiterpene Zealexin A1 from methanol. *ACS Sustain. Chem. Eng.* **2024**, *12*, 12786–12794. doi:10.1021/acssuschemeng.4c02722.
98. Jia M, Liu M, Li J, Jiang W, Xin F, Zhang W, et al. Formaldehyde: an essential intermediate for C1 metabolism and bioconversion. *ACS Synth. Biol.* **2024**, *13*, 3507–3522. doi:10.1021/acssynbio.4c00454.
99. Mohr MKF, Satanowski A, Lindner SN, Erb TJ, Andexer JN. Rewiring *Escherichia coli* to transform formate into methyl groups. *Microb. Cell. Fact.* **2025**, *24*, 55. doi:10.1186/s12934-025-02674-4.
100. Guo Y, Zhang R, Wang J, Qin R, Feng J, Chen K, et al. Engineering yeasts to Co-utilize methanol or formate coupled with CO<sub>2</sub> fixation. *Metab. Eng.* **2024**, *84*, 1–12. doi:10.1016/j.ymben.2024.05.002.
101. Mitic BM, Troyer C, Lutz L, Baumschabl M, Hann S, Mattanovich D. The oxygen-tolerant reductive glycine pathway assimilates methanol, formate and CO<sub>2</sub> in the yeast *Komagataella phaffii*. *Nat. Commun.* **2023**, *14*, 7754. doi:10.1038/s41467-023-43610-7.
102. Tian J, Deng W, Zhang Z, Xu J, Yang G, Zhao G, et al. Discovery and remodeling of *Vibrio natriegens* as a microbial platform for efficient formic acid biorefinery. *Nat. Commun.* **2023**, *14*, 7758. doi:10.1038/s41467-023-43631-2.
103. Kiefer D, Tadele LR, Lilge L, Henkel M, Hausmann R. High-level recombinant protein production with *Corynebacterium glutamicum* using acetate as carbon source. *Microb. Biotechnol.* **2022**, *15*, 2744–2757. doi:10.1111/1751-7915.14138.
104. Kutscha R, Pflügl S. Microbial upgrading of acetate into value-added products—examining microbial diversity, bioenergetic constraints and metabolic engineering approaches. *Int. J. Mol. Sci.* **2020**, *21*, 8777. doi:10.3390/ijms21228777.
105. Nam SH, Ye D-y, Hwang HG, Jung GY. Convergent synthesis of two heterogeneous fluxes from glucose and acetate for high-yield citramalate production. *J. Agric. Food Chem.* **2024**, *72*, 5797–5804. doi:10.1021/acs.jafc.3c09466.
106. Wang P, Li B, Li B, Yang J, Xu X, Yang S-T, et al. Carbon-economic biosynthesis of poly-2-hydrobutanedioic acid driven by nonfermentable substrate ethanol. *Green Chem.* **2022**, *24*, 6599–6612. doi:10.1039/d2gc02480b.
107. Sun M, Gao AX, Liu X, Bai Z, Wang P, Ledesma-Amaro R. Microbial conversion of ethanol to high-value products: Progress and challenges. *Biotechnol. Biofuels Bioprod.* **2024**, *17*, 115. doi:10.1186/s13068-024-02546-w.
108. Qian Z, Yu J, Chen X, Kang Y, Ren Y, Liu Q, et al. *De novo* production of plant 4'-deoxyflavones baicalein and oroxylin A from ethanol in *Crabtree-Negative* yeast. *ACS Syn. Biol.* **2022**, *11*, 1600–1612. doi:10.1021/acssynbio.2c00026.
109. Wang S, Kou T, Varley JB, Akhade SA, Weitzner SE, Baker SE, et al. Cu<sub>2</sub>O/CuS nanocomposites show excellent selectivity and stability for formate generation via electrochemical reduction of carbon dioxide. *ACS Mater. Lett.* **2020**, *3*, 100–109. doi:10.1021/acsmaterialslett.0c00520.
110. Contaldo U, Curtin M, Perard J, Cavazza C, Le Goff A. A pyrene-triazacyclononane anchor affords high operational stability for CO<sub>2</sub>RR by a CNT-supported histidine-tagged CODH. *Angew. Chem. Int. Ed.* **2022**, *61*, e202117212. doi:10.1002/anie.202117212.
111. Tan Z, Tang Z, Wei H, Zhang R, Sun L, Liu W, et al. Helix zipper regulating formolase activity. *ACS Catal.* **2025**, *15*, 1586–1595. doi:10.1021/acscatal.4c07452.
112. Hann EC, Overa S, Harland-Dunaway M, Narvaez AF, Le DN, Orozco-Cárdenas ML, et al. A hybrid inorganic–biological artificial photosynthesis system for energy-efficient food production. *Nat. Food* **2022**, *3*, 461–471. doi:10.1038/s43016-022-00530-x.
113. Li H, Opgenorth PH, Wernick DG, Rogers S, Wu TY, Higashide W, et al. Integrated electromicrobial conversion of CO<sub>2</sub> to higher alcohols. *Science* **2012**, *335*, 1596. doi:10.1126/science.1217643.
114. Lim J, Choi SY, Lee JW, Lee SY, Lee H. Biohybrid CO<sub>2</sub> electrolysis for the direct synthesis of polyesters from CO<sub>2</sub>. *Proc. Natl. Acad. Sci. USA* **2023**, *120*, e2221438120. doi:10.1073/pnas.2221438120.
115. Gong Z, Zhang W, Chen J, Li J, Tan T. Upcycling CO<sub>2</sub> into succinic acid via electrochemical and engineered *Escherichia coli*. *Bioresour. Technol.* **2024**, *406*, 130956. doi:10.1016/j.biortech.2024.130956.



116. Liu G, Zhong Y, Liu Z, Wang G, Gao F, Zhang C, et al. Solar-driven sugar production directly from CO<sub>2</sub> via a customizable electrocatalytic–biocatalytic flow system. *Nat. Commun.* **2024**, *15*, 2636. doi:10.1038/s41467-024-46954-w.
117. Chen K, Zhang P, Chen Y, Fei C, Yu J, Zhou J, et al. Electro-biodiesel empowered by co-design of microorganism and electrocatalysis. *Joule* **2025**, *9*, 101769. doi:10.1016/j.joule.2024.10.001.